

This article was downloaded by:

On: 14 January 2011

Access details: *Access Details: Free Access*

Publisher *Taylor & Francis*

Informa Ltd Registered in England and Wales Registered Number: 1072954 Registered office: Mortimer House, 37-41 Mortimer Street, London W1T 3JH, UK



Molecular Simulation

Publication details, including instructions for authors and subscription information:

<http://www.informaworld.com/smpp/title~content=t713644482>

DNA force-extension curve under uniaxial stretching

Hamid Dalir^a; Takasi Nisisako^b; Yasuko Yanagida^b; Takeshi Hatsuzawa^a

^a Department of Mechano-Micro Engineering, Tokyo Institute of Technology, Tokyo, Japan ^b Precision and Intelligence Laboratory, Tokyo Institute of Technology, Tokyo, Japan

First published on: 27 August 2009

To cite this Article Dalir, Hamid , Nisisako, Takasi , Yanagida, Yasuko and Hatsuzawa, Takeshi(2010) 'DNA force-extension curve under uniaxial stretching', *Molecular Simulation*, 36: 3, 221 — 228, First published on: 27 August 2009 (iFirst)

To link to this Article: DOI: 10.1080/08927020903193812

URL: <http://dx.doi.org/10.1080/08927020903193812>

PLEASE SCROLL DOWN FOR ARTICLE

Full terms and conditions of use: <http://www.informaworld.com/terms-and-conditions-of-access.pdf>

This article may be used for research, teaching and private study purposes. Any substantial or systematic reproduction, re-distribution, re-selling, loan or sub-licensing, systematic supply or distribution in any form to anyone is expressly forbidden.

The publisher does not give any warranty express or implied or make any representation that the contents will be complete or accurate or up to date. The accuracy of any instructions, formulae and drug doses should be independently verified with primary sources. The publisher shall not be liable for any loss, actions, claims, proceedings, demand or costs or damages whatsoever or howsoever caused arising directly or indirectly in connection with or arising out of the use of this material.

DNA force-extension curve under uniaxial stretching

Hamid Dalir^{a1*}, Takasi Nisisako^{b2}, Yasuko Yanagida^{b3} and Takeshi Hatsuzawa^{a4}

^aDepartment of Mechano-Micro Engineering, Tokyo Institute of Technology, 226-8503 Tokyo, Japan; ^bPrecision and Intelligence Laboratory, Tokyo Institute of Technology, 226-8503 Tokyo, Japan

(Received 28 October 2008; final version received 18 July 2009)

Single-molecule experiments indicate that a double-stranded DNA (ds-DNA) increases in length if put under tension greater than 10 pN; beyond this point, its conformation can no longer be described using an inextensible worm-like chain model. For this purpose, a general sequence-dependent elastic model for tensions greater than 10 pN and for both single-stranded (ss) and ds-DNA is proposed, and the effective elastic bending and torsional rigidities are determined from experiments to characterise their deformation. The key to this progress is that the bending and torsional deformations of the DNA backbones, the base-stacking interactions and the hydrogen bond force between the complementary base pairs are quantitatively considered in this model. Moreover, this simple elastic model can be used to globally fit to the abrupt B–S experimental transition data over a wide range of DNA molecule extensions. Based on this robust model, further study may be warranted on the mechanical response of ss- and ds-DNA molecules.

Keywords: double-helical DNA structure; mechanical properties; single-molecule manipulation; base-stacking interactions; hydrogen bond forces

1. Introduction

The DNA molecule is the primary genetic material of most organisms. It is a double-helical biopolymer in which two chains of complementary nucleotides (the subunits whose sequence constitutes the genetic message) wind (usually right-handedly) around a common axis to form a double-helical structure [1]. Because of this unique structure, the elastic property of DNA molecules is a fundamental problem in biological systems [2], and in many of their processes, DNA bending is of particular importance [3]. In fact, a thorough investigation of the deformation and elasticity of DNA will enable us to gain a better understanding of many important biological processes concerned with life and growth [4].

DNA molecules can be stretched by various means including electrostatic, hydrodynamic or magnetic forces. Entropic constrictions have also been employed to stretch DNA molecules by electrostatic forces [5]. To use a magnetic force, magnetic tweezers [6] that use magnetic fields and beads are necessary. Stretching by hydrodynamic force was performed either with free molecular ends or with one end immobilised to a solid surface [7–9]. Most DNA stretching experiments involve anchoring one end of the DNA molecules onto an electrode, bead or other solid surface and stretching the molecule using some type of force. The pioneering experiments by Smith et al. [10] on the mechanical stretching of DNA in a solution indicated that the elasticity of DNA cannot be characterised by the freely jointed chain

(FJC) model that comprises stiff inextensible segments, free to rotate about the joints. Following this, Marko and Siggia [11] introduced their classic elastic model that interpolates between the inextensible worm-like chain (WLC) model and an extensible model for weak and strong extension forces, respectively. A so-called sub-elastic-chain (SEC) model [12] has recently been proposed, considering the development and discussion of more general semiflexible polymer models. Recent experiments supported SEC over WLC as an appropriate model [13]. In another research, Smith et al. [14] examined the elastic properties of single- and double-stranded DNA (ss-DNA/ds-DNA) by stretching the immersed λ -DNA (48 kbp) in the aqueous buffer using the dual-beam optical tweezers system. They observed a sharp structural transition of tension under roughly 65 pN of the freely rotating ds-DNA. It was also revealed that the S-form DNA occurs at the yielding point of the DNA backbone while the freely rotating ds-DNA is stretched [15]. In another study, an analytical worm-like rod chain model for predicting the DNA mechanical response under low stretching force was proposed [16], and its accuracy was then improved in a study by Sarkar et al. [17] by considering free energies of the five DNA states experimentally. The Zhou, Zhang and Ou-Yang model [4], which considers the bending energy and the stacking energy of ds-DNA, can successfully describe the S-form DNA, under high-level stretching, but is not able to represent the structural transition from the B-form DNA to

*Corresponding author. Email: dalir.h.aa@m.titech.ac.jp

the P-form DNA due to its limitation of geometric assumptions [18]. Additionally, all these models neglect the effects of the double-stranded nature of the DNA structure and sequence effects on the ds-DNA mechanics where they should be extremely important to its elastic properties.

Recently, Keten and Buehler [19] reported a simple model that explains the physical mechanism that leads to the breakdown of the WLC idealisation in experiments by using only two generic parameters of the protein domain, the H-bond energy and the protein backbone's persistence length. They showed that a rupture initiation condition characterised by the free energy release rate of H-bonds characterises the limit of the WLC entropic elasticity of β -sheet protein domains and the onset of rupture. Their theoretical framework was quantified and validated for the AFM experiments on I27 [20] (see figure 3 in [19]). They showed that the Bell model [21–25] can be used to predict the strength of subcritical H-bond cluster sizes, as it can also be used to link energy barriers to peak force values (see figure 4 in [19]). However, using the Bell model to calculate force peaks of large clusters of H-bonds requires a homogeneous rupture assumption, which is physically impossible and would indeed lead to excessively high force peaks that approach the strength of covalent bonds. They resolved this controversy by using the energy balance concept from fracture mechanics and applied it to the free energy competition between H-bonds and entropic elasticity of the protein backbone. It was shown that the WLC model alone cannot be used to describe the entire deformation range of protein domains, which is very similar to the problem that we are facing in the study of DNA molecules' elasticity.

In this work, we have studied the parameters affecting DNA elastic mechanical properties considering base-stacking interactions originated from the weak van der Waals attractions between the polar groups of DNA adjacent nucleotide base pairs and the hydrogen bond force between the complementary bases. We have postulated that the double-stranded nature of the DNA structure should be extremely important to its elastic properties, and therefore we have constructed a general elastic model in which this characteristic is properly taken into account. The elastic property of long ds-DNA molecules has then been studied based on atomic force microscopy DNA stretching experiments. Quantitative results have been obtained, and an excellent agreement between theory and the experimental observations has been attained.

2. Elastic model of the DNA molecule

2.1 ss-DNA molecule

As already stressed, the DNA molecule is a double-stranded biopolymer. Its two complementary sugar–phosphate chains

twist around each other to form a right-handed double helix. Each chain is a linear polynucleotide consisting of the following four bases: two purines (A and G) and two pyrimidines (C and T) [1,26]. The two chains are joined together by hydrogen bonds between pairs of nucleotides A-T and G-C. Hereafter, we refer to the two sugar–phosphate chains as the backbones, and the hydrogen-bonded pairs of nucleotides as the base pairs. In this section, we discuss the energetics of such an elastic system for the ss-DNA molecule. First, the energy of the backbones of such double-stranded polymers will be considered; then we will discuss energy terms related to base-stacking and hydrogen bonds.

A general elastic model for the ss-DNA molecule is proposed in Figure 1 (inset), and a structural angle α is introduced to characterise its deformations. The geometry of the DNA backbone is initially assumed based on the B-DNA helix function. For a ss-DNA molecule having radius R , at any point A on the backbone (Figure 1, inset), the force P produces a bending moment $M_b = PR \sin \alpha$ and a torque $M_t = PR \cos \alpha$ about the axes n_1 and n_2 , respectively. We will consider the extension of the ss-DNA molecule on the assumption that it is fixed at the lower end and loaded by an axial load P at the upper end (Figure 1, inset). An element ds between two adjacent points at A is twisted by the torque M_t through the angle

$$d\varphi_t = \frac{M_t}{\tau} ds, \quad (1)$$

where τ is the torsional rigidity of the DNA molecule. Owing to this twist, the upper portion of the DNA backbone rotates about the tangent at A through the angle $d\varphi_t$. This small rotation is represented in Figure 1 (inset) by the vector n_2 along the tangent. It can then be

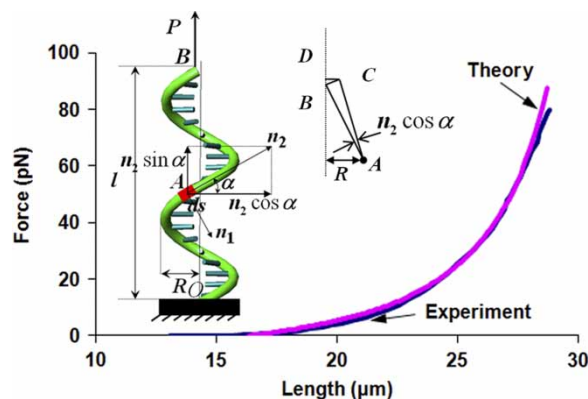


Figure 1. Experimental [14] and theoretical results of single-stranded λ -DNA in blue and red lines, respectively. To match the theoretical and experimental data, the effective elastic bending and torsional rigidities were set to $\sigma_{ss-DNA} = 3.93 \text{ pN nm}^2$ and $\tau_{ss-DNA} = 5.24 \text{ pN nm}^2$, respectively. (Inset) Schematic representation of the ss-DNA parameters used in this paper.

resolved into two components: (1) a rotation $n_2 \cos \alpha$ about a horizontal axis and (2) a rotation $n_2 \sin \alpha$ about a vertical axis. The latter does not produce any extension at the end B . Because of rotation $n_2 \cos \alpha$, point B is displaced to C and we have $\overline{BC} = \overline{AB} n_2 \cos \alpha$. Then, the vertical component of this displacement is

$$\overline{BD} = \overline{BC} \frac{R}{AB} = R n_2 \cos \alpha. \quad (2)$$

Then, the total extension of the end B due to the twist is

$$\text{Ex}_t = \int_0^S R n_2 \cos \alpha, \quad (3)$$

in which the summation is taken along the total length, $S = 21\pi RN / \cos \alpha$, considering the DNA of N base pairs and helical repeat of 10.5 bp, of the ss-DNA from the lower fixed end O to the upper end B .

The extension due to bending can be calculated in the same manner. The angular deflection due to the bending of the element ds by the bending moment M_b is

$$d\varphi_b = \frac{M_b}{\sigma} ds, \quad (4)$$

where σ is the bending rigidity of the DNA molecule. The corresponding rotation of the upper portion of the DNA backbone is shown in Figure 1 (inset) by the vector n_1 . In the same manner as for the extension caused by torque M_t , it can be shown that only its horizontal component $n_1 \sin \varphi$ contributes to the vertical extension of the end B , and that the magnitude of this extension is

$$\text{Ex}_b = \int_0^S R n_1 \sin \alpha. \quad (5)$$

By adding Equations (3) and (5), the total extension of the end B becomes

$$\text{Ex}_{ss} = \text{Ex}_t + \text{Ex}_b = \int_0^S R(n_2 \cos \alpha + n_1 \sin \alpha). \quad (6)$$

Substituting Equation (1) for n_2 and Equation (4) for n_1 , we obtain

$$\text{Ex}_{ss} = \int_0^S R \left(\frac{M_t}{\tau} \cos \alpha + \frac{M_b}{\sigma} \sin \alpha \right) ds. \quad (7)$$

In order to obtain the value of α at a given stretching force, the discrete persistent chain (DPC) model [27] is used having the following Hamiltonian:

$$H = \sum_i \left[\frac{J}{2} \Theta_{i,i+1}^2 - b \vec{P} \cdot \hat{t}_i \right]. \quad (8)$$

Here, \hat{t}_i is the i th bond orientation, b is the (fixed) bond

length, $\Theta_{i,i+1}$ is the angle between the i th and $(i+1)$ th bonds (i.e. $\cos \Theta_{i,i+1} = \hat{t}_i \cdot \hat{t}_{i+1}$) and \vec{P} is the external stretching force. Interestingly, two other common WLC and FJC models can be obtained from DPC Hamiltonian, by taking limits of zero bond length (WLC) or zero coupling J (FJC). Here, we consider a generalised DPC model that considers the torsional angles per nucleotide of the backbone conformation of ss-DNA and the valent angles having values different from 180° , which is not considered in the WLC and traditional DPC models. For this, a chain whose ground state is in a zigzag (all-*trans*) configuration is introduced as

$$H = \sum_i \left[\frac{J}{2} (\Theta_{i,i+1} + (-1)^i \Theta_0 \cos \Psi_{i,i+1})^2 - b \vec{P} \cdot \hat{t}_i \right]. \quad (9)$$

Here, Ψ_i is the torsional angle associated with the rotation of the i th bond. For simplicity, we assign the same preferred angle Θ_0 to each bond pair.

In order to simplify the problem of the 'zigzag' chain, we map the model back onto the DPC model, with renormalised parameters. Let us consider a chain consisting of only odd (or only even) nodes of the zigzag (i.e. $\dots - "i" - "i+2" - "i+4" - \dots$). The ground state of this chain is a straight line, but the bond length (even without thermal fluctuation) is a function of the applied force: $b^* = 2b \cos \theta^*$, where $\theta^*(f)$ is the preferred bond orientation angle θ_i , with respect to the direction of \vec{P} . Therefore, Equation (9) can be rewritten as

$$H = \sum_i \left[\frac{J}{2} (2\theta^* - \Theta_0)^2 - f b \cos \theta^* \right]. \quad (10)$$

In the ground-state configuration (i.e. zigzag, $\theta_i = (-1)^i \theta^*$), the value of θ^* may be obtained by minimising the Hamiltonian at a given stretching force as

$$\begin{aligned} \theta^*(P) = (Pb)^{-1/3} [6J\Theta_0 + 2\xi^{1/2}]^{1/3} + (8J + 2Pb) \\ \times (Pb)^{-2/3} [-6J\Theta_0 + 2\xi^{1/2}]^{-1/3}, \end{aligned} \quad (11)$$

where $\xi = -128P^{-1}b^{-1}J^3 - (96 - 9\Theta_0^2)J^2 - 24PbJ - 2P^2b^2$ and $J = (kT)b^{-1}l_p$ can be determined by measuring the experimentally observable persistence length l_p . Therefore, Equation (7) can be rewritten as

$$\text{Ex}_{ss} \approx \int_0^S \frac{PS^2 \sin^2 \theta^*}{441 \pi^2 N^2} \left(\frac{\sin^2 \theta^*}{\tau_{ss\text{-DNA}}} + \frac{\cos^2 \theta^*}{\sigma_{ss\text{-DNA}}} \right) ds. \quad (12)$$

The experimental results of ss-DNA in the phosphate buffer [14] were used as a benchmark to determine the unknown effective parameters of the elastic backbone. The experimental and theoretical results are shown as the blue and red lines in Figure 1, respectively. The same parameters as in the traditional WLC models were assumed: b (which is fixed at its physical value of a

typical chemical bond length, 0.1 nm) and ss-DNA persistence length $l_p \approx 0.85$ nm (extracted from the moderate force stretching behaviour). To match the theoretical and experimental data, the effective bending and torsional rigidities and the preferred angle to each bond pair were set to $\sigma_{ss-DNA} = 3.93$ pN nm², $\tau_{ss-DNA} = 5.24$ pN nm² and $\Theta_0 = 50^\circ$, respectively. These effective parameters are slightly larger than the expected ones, which are mainly due to the effects of the buffer solution and the ions on the ss-DNA molecules stretching. To check the sensitivity of the proposed ss-DNA model with respect to the parameters that feed into Equation (12), degrees-of-freedom adjusted *R*-square criterion is used. The residual degrees of freedom is defined as the number of response values minus the number of fitted coefficients estimated from the response values. Therefore, it shows the number of independent pieces of information involving the data points that are required to calculate the sum of squares. Note that if parameters are bounded and one or more of the estimates are at their bounds, then those estimates are regarded as fixed. The adjusted *R*-square statistics can take on any value less than or equal to 1, with a value closer to 1 indicating a better fit. For example, for a set of $\sigma_{ss-DNA} = 3.93$ pN nm², $\tau_{ss-DNA} = 5.24$ pN nm² and $\Theta_0 = 50^\circ$, adjusted *R*-square value of 0.9996 is obtained, which means that the fit explains 99.96% of the total variation in the data about the average. However, considering two very near sets of $\sigma_{ss-DNA} = 3.92$ pN nm², $\tau_{ss-DNA} = 5.23$ pN nm², $\Theta_0 = 50^\circ$ and $\sigma_{ss-DNA} = 3.94$ pN nm², $\tau_{ss-DNA} = 5.24$ pN nm², $\Theta_0 = 50^\circ$ will lead to the adjusted *R*-square values of 0.9537 and 0.9641, respectively. This shows that small amounts of the total variation in the data are about the average, indicating that the values of σ_{ss-DNA} and τ_{ss-DNA} should be determined quite carefully.

2.2 ds-DNA molecule

Before constructing the ds-DNA mechanical model, we should discuss another kind of important interactions; namely, the base-stacking interaction between adjacent nucleotide base pairs [1,26] and hydrogen bond interaction between the complementary bases [28].

2.2.1 Base-stacking interactions between the base pairs

Base-stacking interactions originate from the weak van der Waals attraction between the polar groups in adjacent nucleotide base pairs. Such interactions are short-ranged, and their total effect is usually described by a potential energy of the Lennard-Jones form (6–12 potential [1]), which contributes significantly to the stability of the double helix. In a continuum theory of elasticity, the total base-stacking potential energy can be converted into the

form of the integration [4]:

$$U_{bs} = \int_0^S \frac{\varepsilon}{r_0} \left[\left(\frac{\sin \alpha_0}{\sin \alpha} \right)^{12} - 2 \left(\frac{\sin \alpha_0}{\sin \alpha} \right)^6 \right] ds, \quad (13)$$

for $\alpha \leq \pi/2$,

where $r_0 = S/N$ is the backbone arclength between the adjacent bases; α_0 is related to the equilibrium distance between a DNA dimer ($r_0 \sin \alpha_0 \approx 3.4$ Å) and ε is the base-stacking intensity which, in the average sense, can be considered as a constant, with $\varepsilon \approx 14.0 k_B T$ averaged over quantum mechanically calculated results on all the different DNA dimers [4]. Figure 2(a) shows the Lennard-Jones form of base-stacking energy and stiffness, $k_{bs} = \partial^2 U_{bs} / \partial l^2$, via the Crotti–Engesser theorem [29].

2.2.2 Hydrogen bond force between the complementary bases

The hydrogen bond force is the interaction between the complementary bases. Moreover, the GC base pair has three hydrogen bonds and AT has two. In the ds-DNA mechanical modelling, the three/two hydrogen bonds in GC/AT are replaced by only one virtual spring, with the axial and torsional stiffness as a function of the distance (R_i) and the angle (θ_{iHj}) between the donor and the acceptor. The single hydrogen bond energy could be expressed by the CHARMM-like potential [28,30,31], which slightly underestimates the overall experimentally measured values [32] as

$$E(R_i, \theta) = \sum_{R_{ij}} A D_0 \left[5 \left(R_0 / R_i \right)^{12} - 6 \left(R_0 / R_i \right)^{10} \right] \cos^4 \theta_{iHj}, \quad (14)$$

where D_0 represents the hydrogen bond energy intensities. Furthermore, we assume that the distances of the hydrogen bonds are the same along the ds-DNA molecule, the B-form DNA has the lowest hydrogen bond potential, D–H–A is a straight line and the hydrogen atom is always at the centre of the hydrogen bond at the initial state. Through the Crotti–Engesser theorem [29], the axial and twisting stiffness due to the reaction forces and bending moments could be expressed as

$$k_j = \sum_i C_{j,i} \frac{\partial^2}{\partial x_i^2} E(R_0 + dx_i, \theta_0 + d\theta_i), \quad (15)$$

where i, j and $C_{j,i}$ represent the number of hydrogen bonds, different kinds of reaction forces/bending moments/torques, and weighting coefficients, respectively. The x_j and θ_j are the displacement along the hydrogen bond direction and the angle between the donor and the

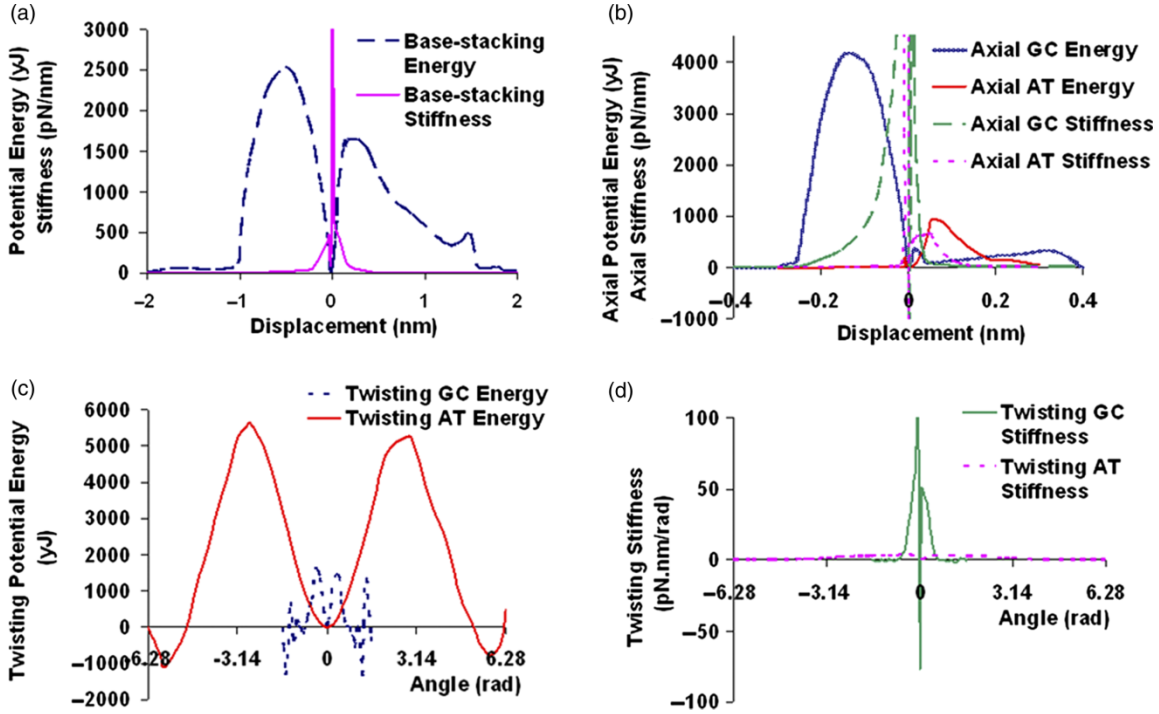


Figure 2. The stiffness of the virtual elements. (a) The base-stacking energy and stiffness of the virtual springs between the complementary base pairs of the ds-DNA molecule. (b)–(d) The AT and GC hydrogen bond axial and torsional energy and stiffness plots.

acceptor, respectively. Equation (13) is presented as Figure 2(b)–(d).

2.2.3 Mechanical model

Considering the effects of base-stacking interactions and hydrogen bond forces, the total energy of a ds-DNA molecule under the action of an external force (Figure 3(a)) is expressed as

$$U_{ds} = U_{backbone} + U_{bs} + U_{Ahb} + U_{Thb}, \quad (16)$$

where

$$U_{backbone} \approx \int_0^S (P^2 S^2 \cos^2 \alpha / 1764 \pi^2 N^2) (\cos^2 \alpha / \tau_{ds-DNA} + \sin^2 \alpha / \sigma_{ds-DNA}) ds$$

is the ds-DNA backbone energy; U_{bs} is the total base-stacking potential energy along all the adjacent nucleotide base pairs and can be expressed as

$$U_{bs} = \int_0^{Ex_{ds}/(N-1)} 2k_{bs} \xi (N-1) d\xi, \quad (17)$$

where ξ is the distant change between two adjacent nucleotides and Ex_{ds} is the total extension of the ds-DNA molecule. Furthermore, the total hydrogen bond energy

caused by the variations in distance and angle between the donor and the acceptor can be defined as

$$U_{hb} = 4N_{GC} \left[\int_0^{R_f - R_0} k_{A-GC} R \cdot dR + \int_0^{\alpha_f - \alpha_0} k_{T-GC} \alpha \cdot d\alpha \right] + 4N_{AT} \left[\int_0^{R_f - R_0} k_{A-AT} R \cdot dR + \int_0^{\alpha_f - \alpha_0} k_{T-AT} \alpha \cdot d\alpha \right], \quad (18)$$

where N_{GC} and N_{AT} are the number of GC and AT base pairs in the ds-DNA sequence, respectively. R_0 , R_f , α_0 and α_f are the initial and final values of ds-DNA radius R and structural angle α , respectively, and k_{A-GC} , k_{T-GC} , k_{A-AT} and k_{T-AT} are the axial and torsional GC and AT hydrogen bond stiffnesses, respectively. Since $\sin \alpha = l/S$, where l is the length of the ds-DNA molecule, one can obtain

$$\alpha \cdot d\alpha = \left[(S^2 - l^2)^{-0.5} \sin^{-1} \frac{l}{S} \right] dl. \quad (19)$$

Moreover, from $2l\pi RN = S \cos \alpha$, we have

$$R \cdot dR = \frac{-l}{441 \pi^2 N^2} dl. \quad (20)$$

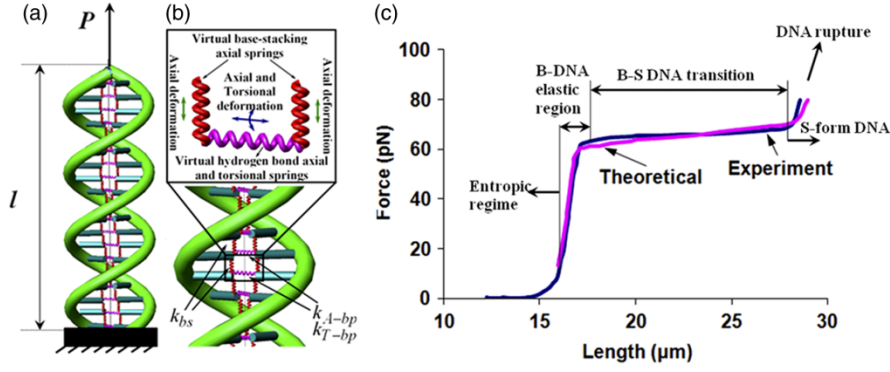


Figure 3. (a) Schematic representation of the ds-DNA geometry and loading conditions. (b) The location of virtual springs in the ds-DNA mechanical model. Springs parallel and perpendicular to the DNA axis represent the equivalent base-stacking and hydrogen bond interaction forces between the complementary bases along the ds-DNA double helix, respectively, and (c) good agreement was achieved between the theoretical (red line) and the experimental (blue line) results [14] for the applied forces larger than ~ 10 pN via considering the effective elastic bending and torsional rigidities as $\sigma_{\text{ds-DNA}} = 210 \text{ pN nm}^2$ and $\tau_{\text{ds-DNA}} = 370 \text{ pN nm}^2$, respectively. From 10 pN and up to about 80 pN, DNA stretches elastically as does any material, i.e. following Hooke's law. At about 65 pN, a surprising cooperative transition occurs and the DNA stretches to about 1.8 times its crystallographic length with a small change in applied force P .

Based on Equations (18–20), we can write that

$$U_{\text{Ahb}} = \frac{1}{110\pi^2 N} \int_0^{\text{Ex}_{\text{ds}}} [((N_{\text{GC}}/N)k_{\text{A-GC}} + (1 - N_{\text{GC}}/N)k_{\text{A-AT}})l]dl \quad (21)$$

and

$$U_{\text{Thb}} = \int_0^{\text{Ex}_{\text{ds}}} [(N_{\text{GC}}k_{\text{T-GC}} + (1 - N_{\text{GC}})k_{\text{T-AT}}) \times (4(S^2 - l^2)^{-0.5} \sin^{-1}(l/S))]dl, \quad (22)$$

where U_{Ahb} and U_{Thb} are the axial and torsional components of the total hydrogen bond energies caused by the variations in distance and angle between the donor and the acceptor, respectively. Because the GC and AT base pairs have three and two hydrogen bonds, respectively, the ds-DNA sequence information has been embedded into the ds-DNA mechanical model based on Equation (16). From the analysis made up to this point, the total energy of a ds-DNA molecule under the action of a stretching force can be expressed as

$$U_{\text{ds}} = \int_0^S \left\{ \frac{P^2(S^2 - l^2)}{1764\pi^2 S^2 N^2} \left(\frac{S^2 - l^2}{\tau_{\text{ds-DNA}}} + \frac{l^2}{\sigma_{\text{ds-DNA}}} \right) + \frac{\varepsilon}{r_0} \left[\left(\frac{S \sin \alpha_0}{l} \right)^{12} - 2 \left(\frac{S \sin \alpha_0}{l} \right)^6 \right] + \partial_s \int_0^{\text{Ex}_{\text{ds}}} \left[\left(4N(S^2 - l^2)^{-0.5} \sin^{-1}(l/S) \right) \left(\frac{N_{\text{GC}}}{N} k_{\text{T-GC}} + \left(1 - \frac{N_{\text{GC}}}{N} \right) k_{\text{T-AT}} \right) + \frac{l}{110\pi^2 N} \left(\frac{N_{\text{GC}}}{N} k_{\text{A-GC}} + \left(1 - \frac{N_{\text{GC}}}{N} \right) k_{\text{A-AT}} \right) \right] dl \right\} ds. \quad (23)$$

To obtain the average extension of the ds-DNA central axis, the Green equation, $\partial_S \Omega(l; S) = \hat{M} \Omega(l; S)$, for a polymer whose energy is expressed in the form of Equation (23), is considered, where $\Omega(l; S)$ is the wave function and

$$\hat{M} = \int_0^{\text{Ex}_{\text{ds}}} \left\{ \left(6N(S^2 - l^2)^{-1} (1 + l(S^2 - l^2)^{-0.5} \sin^{-1}(l/S)) \right) \times \left(\frac{N_{\text{GC}}}{N} k_{\text{T-GC}} + \left(1 - \frac{N_{\text{GC}}}{N} \right) k_{\text{T-AT}} \right) + \frac{1}{73\pi^2 N} \left\{ \left[\left(\frac{N_{\text{GC}}}{N} k_{\text{A-GC}} + \left(1 - \frac{N_{\text{GC}}}{N} \right) k_{\text{A-AT}} \right) \right] \partial_l \right. \right. \right. \\ \left. \left. - \frac{P^2(S^2 - l^2)}{1764(k_B T) \pi^2 S^2 N^2} \left(\frac{S^2 - l^2}{\tau_{\text{ds-DNA}}} + \frac{l^2}{\sigma_{\text{ds-DNA}}} \right) - \frac{\varepsilon}{r_0(k_B T)} \left[\left(\frac{S \sin \alpha_0}{l} \right)^{12} - 2 \left(\frac{S \sin \alpha_0}{l} \right)^6 \right] \right\} \right\} \quad (24)$$

is Hermitian and can be diagonalised by unitary matrix.

Therefore, the total free energy of ds-DNA chains can be expressed as

$$E_f = S(k_B T) \eta, \quad (25)$$

where η is the ground-state eigenvalue of the above-mentioned Green equation, $\partial_S \Omega(l; S) = \hat{M} \Omega(l; S)$, and can be obtained numerically through the standard diagonalisation method. Consequently, the averaged dielectrophoretic extension of a ds-DNA can be calculated as

$$\langle \text{Ex}_{\text{ds}} \rangle = \partial_P E_f = S(k_B T) \partial_P \eta. \quad (26)$$

Turning to the experimental data shown in Figure 3 and to match the theoretical stretching results with those of

experiments, the effective bending and torsional rigidities of the ds-DNA molecule were set to $\sigma_{\text{ds-DNA}} = 210 \text{ pN nm}^2$ and $\tau_{\text{ds-DNA}} = 370 \text{ pN nm}^2$, respectively, having an adjusted R -square value of 0.9748. It should be noted that slight changes in the values of $\sigma_{\text{ds-DNA}}$ and $\tau_{\text{ds-DNA}}$ will lead to the smaller adjusted R -square values and, consequently, less amounts of the total variation in the data will be about the average.

As it can be seen from these calculations, the double helix structure of ds-DNA makes it a very stiff molecule with base pairs stacked in a highly ordered manner. In contrast, ss-DNA is a far more flexible polymer creating a much tighter random coil configuration that leads to strong intramolecular interactions; further, ss-DNA presents unpaired bases, which can bind both locally, to create hairpins, or with distal regions, creating complex higher-order structures.

To obtain a more detailed understanding of the sequence-dependent mechanical properties of DNA molecules, we investigated synthetic constructs of double-stranded poly(dG-dC) as well as poly(dA-dT) and combinations with different $N_{\text{GC}}/N_{\text{AT}}$ ratios. Considering Equation (26), the extension traces were recorded where the molecules having the same total number of base pairs (N) but different ratios of $N_{\text{GC}}/N_{\text{AT}}$ ranging from 0 to ∞ were stretched up to about 1.8 times of their crystallographic lengths (Figure 4). The different sequences exhibit pronounced differences in their conformational transitions. For double-stranded poly(dA-dT) ($N_{\text{GC}}/N_{\text{AT}} = 0$), the B–S transition occurs at 35 pN (nearly 50% of that of λ -DNA), which is due to the fact that the mechanical energy deposited in the double strand during stretching reaches the backbone torsional energy at lower forces due to the lower energy absorbance capacity of AT base pairs. However, as the ratio of $N_{\text{GC}}/N_{\text{AT}}$

increases towards infinity, AT base pairs are replaced with GC ones and base pairs will be capable of absorbing larger part of the mechanical energy, and therefore the B–S transition occurs at higher applied forces (e.g. 55 pN for $N_{\text{GC}}/N_{\text{AT}} = 0.5$, 65 pN for $N_{\text{GC}}/N_{\text{AT}} = 1.0$ (λ -DNA molecules); 70 pN for $N_{\text{GC}}/N_{\text{AT}} = 2.0$ and 75 pN for $N_{\text{GC}}/N_{\text{AT}} = \infty$), as can be seen from Figure 4.

3. Results and discussion

In the simulation, a prescribed displacement is applied to the free end of the freely rotating ds-DNA molecule. The mechanical ds-DNA model is then solved based on Equation (26) (Figure 3(c)). A good agreement was achieved between the numerical and the experimental results [21], considering that the information of ds-DNA at low applied forces (under $\sim 10 \text{ pN}$) is ignored because the mechanical characteristics at large applied forces (10–80 pN) are focused. When the applied forces are lower than $\sim 10 \text{ pN}$ (entropic regime), the molecule behaves as an ideal (WLC) polymer of persistence length $l_p \approx 50 \text{ nm}$. Its elastic behaviour is purely due to a reduction of its entropy upon stretching. From 10 pN and up to about 80 pN, DNA stretches elastically as does any material (Figure 3(c)), i.e. following Hooke's law: $F \approx E x_{\text{ds}}$ (where $E x_{\text{ds}} = l - l_0$ is the increase in the length of the molecule of initial length l_0). However, at about 65 pN, a surprising transition occurs, where DNA stretches to about 1.8 times of its crystallographic length. This transition is highly cooperative, i.e. a small change in force results in a large change in extension. To address the possible structural modification in the results of DNA molecule stretching, three stages are considered here.

When the external applying force is in the range of 10–65 pN (first stage), the energy required for twisting the complementary base pairs is higher than the backbone's bending and torsional energies, and part of the work done by the external force acting on the chain is accumulated in the base-stacking and hydrogen bond's virtual springs (Figure 3(a),(b)). As the applied force is more increased (second stage), the virtual base-stacking springs release most of their absorbed energy because the distance between the adjacent base pairs exceeds the limitation. This will enforce the base pairs and the backbones to store more energy, which causes the torque of the ds-DNA local structure to overcome the backbone torsional rigidity and the B–S conformational transition occurs. The exact structure of the new ds-DNA molecule, which is indeed $\sim 80\%$ longer than B-DNA, depends on which extremities of the DNA are being pulled ($3' - 3'$ or $5' - 5'$). If both $3'$ extremities are being pulled, the double helix unwinds upon stretching, but in the case of pulling both $5'$ ends, the helical structure is preserved and characterised by a strong base pair inclination, a narrower minor groove and a diameter of roughly 30% less than that of B-DNA [33].

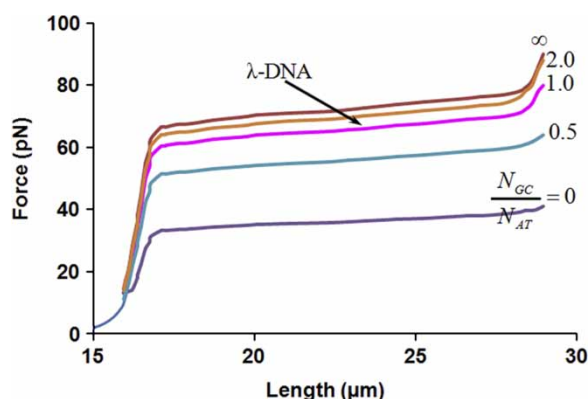


Figure 4. The mechanical compliance of DNA strongly depends on the specific base pairing in the double helix. For double-stranded poly(dA-dT) DNA, the B–S transition occurs at 35 pN, nearly half of that of λ -DNA ($N_{\text{GC}}/N_{\text{AT}} = 1$), while in poly(dG-dC) the force of the B–S transition is raised to 75 pN, which is slightly larger than that for λ -DNA.

In both cases, if the loading further increases (third stage), the backbones are forced to absorb more energy by stretching as an S-form DNA double helix in a linear manner (Hooke's law). Rupture of the molecule (by unpairing of the bases) has been predicted to occur, as the extension is more than twice that of B-DNA [34,35].

4. Conclusions

In this paper, we constructed an elastic mechanical model for both the ss- and ds-DNA molecules through experimental single-molecule manipulation. The key to this progress was that the bending and torsional deformations of the DNA backbones, the base-stacking interactions and the hydrogen bond force between the complementary base pairs were quantitatively considered in this model. A general sequence-dependent elastic model for both single- and double-stranded biopolymers was proposed, and the effective bending and torsional rigidities were determined to characterise their deformation. Based on this robust model, further study may be warranted on the mechanical response of ss- and ds-DNA molecules.

Notes

1. Mailing Address: R2-6, 4259 Nagatsuta-cho, Midori-ku, Yokohama, Kanagawa 226-8503, Japan. Tel./Fax: +81-45-924-5088.
2. Email: nisisako@pi.titech.ac.jp
3. Email: yanagida@pi.titech.ac.jp
4. Email: hat@pi.titech.ac.jp

References

- [1] W. Saenger, *Principles of Nucleic Acid Structure*, Springer-Verlag, New York, 1984.
- [2] B. Alberts, D. Bray, J. Lewis, M. Raff, K. Roberts, and J.D. Watson, *The Molecular Biology of the Cell*, Garland, New York, 1994.
- [3] J. Widom, *Role of DNA sequence in nucleosome stability and dynamics*, Q. Rev. Biophys. 34 (2001), pp. 269–324.
- [4] H. Zhou, Y. Zhang, and Z. Ou-Yang, *Elastic property of single double-stranded DNA molecules: Theoretical study and comparison with experiments*, Phys. Rev. E 62 (2000), pp. 1045–1058.
- [5] S.W. Turner, M. Cabodi, and H.G. Craighead, *Confinement-induced entropic recoil of single DNA molecules in a nanofluidic structure*, Phys. Rev. Lett. 88 (2002), pp. 128103.1–128103.4.
- [6] C. Gosse and V. Croquette, *Magnetic tweezers: Micromanipulation and force measurement at the molecular level*, Biophys. J. 82 (2002), pp. 3314–3329.
- [7] J. Allemand, D. Bensimon, L. Jullien, A. Bensimon, and V. Croquette, *pH-dependent specific binding and combing of DNA*, Biophys. J. 73 (1997), pp. 2064–2070.
- [8] O. Bakajin, T. Duke, C. Chou, S. Chan, R. Austin, and E. Cox, *Electrohydrodynamic stretching of DNA in confined environments*, Phys. Rev. Lett. 80 (1998), pp. 2737–2740.
- [9] D. Bensimon, A.J. Simon, V. Croquette, and A. Bensimon, *Stretching DNA with a receding meniscus: Experiments and models*, Phys. Rev. Lett. 74 (1995), pp. 4754–4757.
- [10] S.B. Smith, L. Finci, and C. Bustamante, *Direct mechanical measurements of the elasticity of single DNA molecules by using magnetic beads*, Science 258 (1992), pp. 1122–1126.
- [11] J.F. Marko and E.D. Siggia, *Stretching DNA*, Macromolecules 28 (1995), pp. 8759–8770.
- [12] P.A. Wiggins and P.C. Nelson, *Generalized theory of semiflexible polymers*, Phys. Rev. E 73 (2006), pp. 031906.1–031906.13.
- [13] P.A. Wiggins, T.V. Heijden, F.M. Herrero, A. Spakowitz, R. Phillips, J. Widom, C. Dekker, and P.C. Nelson, *High flexibility of DNA on short length scales probed by atomic force microscopy*, Nature Nanotechnol. 1 (2006), pp. 137–141.
- [14] S.B. Smith, Y. Cui, and C. Bustamante, *Overstretching B-DNA: The elastic response of individual double-stranded and single-stranded DNA molecules*, Science 271 (1996), pp. 795–799.
- [15] J.F. Leger, G. Romano, A. Sarkar, J. Robert, L. Bourdieu, D. Chatenay, and J.F. Marko, *Structural transitions of a twisted and stretched DNA molecule*, Phys. Rev. Lett. 83 (1999), pp. 1066–1069.
- [16] C.J. Benham, *Onset of writhing in circular elastic polymers*, Phys. Rev. A 39 (1989), pp. 2582–2586.
- [17] A. Sarkar, J.F. Leger, D. Chatenay, and J.F. Marko, *Structural transitions in DNA driven by external force and torque*, Phys. Rev. E 63 (2001), pp. 051903.1–051903.10.
- [18] K.N. Chiang, C.A. Yuan, C.N. Han, and C.Y. Chou, *Mechanical characteristic of ss-DNA/ds-DNA molecule under external loading*, Appl. Phys. Lett. 88 (2006), pp. 023902.1–023902.3.
- [19] S. Keten and M.J. Buehler, *Strength limit of entropic elasticity in beta-sheet protein domains*, Phys. Rev. E 78 (2008), pp. 061913.1–061913.7.
- [20] P.E. Marszalek, H. Lu, H.B. Li, M.C. Vazquez, A.F. Oberhauser, K. Schulten, and J.M. Fernandez, *Mechanical unfolding intermediates in titin modules*, Nature 402 (1999), pp. 100–103.
- [21] G.I. Bell, *Models for the specific adhesion of cells to cells*, Science 200 (1978), pp. 618–627.
- [22] T. Ackbarow, X. Chen, S. Keten, and M.J. Buehler, *Hierarchies, multiple energy barriers, and robustness govern the fracture mechanics of α -helical and β -sheet protein domains*, Proc. Natl Acad. Sci. USA 104 (2007), pp. 16410–16415.
- [23] E. Evans and K. Ritchie, *Dynamic strength of molecular adhesion bonds*, Biophys. J. 72 (1997), pp. 1541–1555.
- [24] R. Merkel, P. Nassoy, A. Leung, K. Ritchie, and E. Evans, *Energy landscapes of receptor–ligand bonds explored with dynamic force spectroscopy*, Nature 397 (1999), pp. 50–53.
- [25] M. Rief, J.M. Fernandez, and H.E. Gaub, *Elastically coupled two-level systems as a model for biopolymer extensibility*, Phys. Rev. Lett. 81 (1998), pp. 4764–4767.
- [26] J.D. Watson, N.H. Hopkins, J.W. Roberts, J.A. Steitz, and A.M. Weiner, *Molecular Biology of the Gene*, 4th ed., Benjamin/Cummings, Menlo Park, CA, 1987.
- [27] C. Storm and P.C. Nelson, *Theory of high-force DNA stretching and overstretching*, Phys. Rev. E 67 (2003), pp. 051906.1–051906.12.
- [28] G.A. Jeffery and W. Saneger, *Hydrogen Bonding in Biological Structures*, 1st ed., Springer, Berlin, 1994.
- [29] A.C. Ansel and S.K. Fenster, *Strength and Applied Elasticity*, 4th ed., Prentice-Hall, Upper Saddle River, NJ, 2003.
- [30] S.L. Mayo, B.D. Olafson, and W.A. Goddard, *DREIDING: A generic force field for molecular simulations*, J. Phys. Chem. 94 (1990), pp. 8897–8909.
- [31] B.R. Brooks, R.E. Bruccoleri, B.D. Olafson, D.J. States, S. Swaminathan, and M.J. Karplus, *CHARMM: A program for macromolecular energy, minimization, and dynamics calculations*, Comput. Chem. 4 (1983), pp. 187–217.
- [32] R.M. Wachter and B.P. Branchaud, *Molecular modeling studies on oxidation of hexopyranoses by galactose oxidase. An active site topology apparently designed to catalyze radical reactions, either concerted or stepwise*, J. Am. Chem. Soc. 118 (1996), pp. 2782–2789.
- [33] A. Lebrun and R. Lavery, *Modelling extreme stretching of DNA*, Nucleic Acids Res. 24 (1996), pp. 2260–2267.
- [34] M. Wilkins, R. Gosling, and W. Seeds, *Physical studies of nucleic acid: Nucleic acid: An extensible molecule?* Nature 167 (1951), pp. 759–760.
- [35] A. Bensimon, A. Simon, A. Chiffaudel, V. Croquette, F. Heslot, and D. Bensimon, *Alignment and sensitive detection of DNA by a moving interface*, Science 265 (1994), pp. 2096–2098.